Applications of Temperature Dependent Paramagnetic Properties for Quantifying Mineral Content and Extending the Use of Paramagnetic Dopants for Laboratory or Borehole Analysis of NMR Data

Cody W. Good and *David K.* Potter*

Department of Physics, University of Alberta, Edmonton, Alberta, T6G 2E1, Canada

Abstract. Firstly, we extend previous work [1, 2] on the theoretical modelling of the temperature dependence of the magnetic susceptibility of paramagnetic minerals, and how this can be used to quantify paramagnetic mineral content from temperature dependent magnetic susceptibility measurements on core samples in the laboratory, or from borehole magnetic susceptibility data. We will further show the effects of porosity and fluid type within the pores on the results. Mass magnetic susceptibility is less dependent on porosity than volume magnetic susceptibility, and is potentially more useful for mineral quantification in the laboratory where the mass of core samples can easily be measured. Borehole sensors, however, measure volume magnetic susceptibility, since the mass of the formation rock is not measured (though it can be estimated from bulk density log data). Furthermore, we will show how low temperature measurements increase the paramagnetic signal, which is particularly useful for quantifying extremely small amounts of paramagnetic minerals in core samples in the laboratory. Secondly, recent work by Mitchell et al [3] showed how the addition of a paramagnetic dopant (in aqueous form) to the brine phase of a carbonate reservoir sample could be used to improve the separation of the brine from the oil NMR T2 relaxation time peaks in the laboratory at room temperature. The effect was shown to be dependent upon the concentration of the dopant. Our present study shows how modelling the temperature dependent paramagnetic susceptibility of the dopant can potentially be used to predict how such a paramagnetic dopant would behave with depth in a borehole for in-situ applications. Since the paramagnetic susceptibility of the dopant decreases with increasing temperature, we show how the paramagnetic susceptibility signal could potentially be used as a proxy for "effective paramagnetic molar concentration" values of the dopant at different temperatures. This could potentially broaden the applicability of Mitchell et al's [3] technique to a borehole setting. Also, since the dopant's paramagnetic susceptibility signal increases with decreasing temperature (thus increasing its "effective paramagnetic molar concentration"), then laboratory NMR T2 time measurements taken at temperatures slightly lower than room temperature could further improve the separation of the brine and oil peaks compared to Mitchell et al's [3] room temperature measurements.

1 Introduction

One motivation for this study was to extend the theoretical modelling of the temperature dependence of magnetic susceptibility of samples that contain a paramagnetic mineral. This would produce theoretical curves of magnetic susceptibility with temperature that could subsequently be used to provide a means of quantifying the paramagnetic mineral content by comparing with laboratory heating or cooling magnetic susceptibility measurements, or by comparing with borehole magnetic susceptibility data. The magnetic susceptibility of paramagnetic minerals such as illite is temperature dependent (as described in the theory and methods **section 2** below), whereas the magnetic susceptibility of diamagnetic minerals such as quartz is independent of temperature. Some preliminary modelling was previously undertaken [1, 2] but was restricted to mass magnetic susceptibility. Now we also show modelling for volume magnetic susceptibility, since this is measured by borehole magnetic susceptibility tools measure as the sensor does not take account of the mass of the formation rock (although the volume magnetic susceptibility values could potentially be converted to mass magnetic susceptibility using the bulk density log data). In the present study we also model the effects of low temperature, as well as porosity and pore fluid type on both the volume magnetic susceptibility and the mass magnetic susceptibility.

Increasing temperature causes the magnetic susceptibility of paramagnetic minerals to decrease. Thus temperature dependent magnetic susceptibility measurements in the laboratory can be used to provide a sensitive means of identifying the presence of

* Corresponding author: dkpotter@ualberta.ca

paramagnetic minerals. Theoretical curves of temperature dependent magnetic susceptibility for single minerals or mineral mixtures can be used to quantify the paramagnetic mineral content in relatively simple systems, even in rocks with a very low paramagnetic mineral content and a high diamagnetic mineral content. The mineral mixture curves can also simultaneously quantify the diamagnetic mineral content in relatively simple systems. A further beneficial consequence of the temperature dependence of paramagnetic minerals is that cooling a rock core sample increases the paramagnetic susceptibility signal, so that extremely small amounts of a paramagnetic mineral or minerals in a rock can be identified at low temperature even if they are not apparent from traditional room temperature measurements.

It is particularly important to take account of the temperature dependence of paramagnetic minerals in order to obtain reliable paramagnetic mineral content estimates from borehole magnetic susceptibility data, since temperature and thus magnetic susceptibility varies with depth. This potentially allows a means of estimating in-situ paramagnetic mineral content.

A second motivation for this study was influenced by a recent paper [3] which demonstrated how the addition of a paramagnetic dopant (manganese chloride, $MnCl_2$, in aqueous form) to the brine phase of a carbonate reservoir sample could be used to improve the separation between the brine and the oil NMR T2 peaks in the laboratory at room temperature. The effect was dependent upon the concentration of the dopant. Since the paramagnetic susceptibility of the manganese chloride dopant should decrease with increasing temperature, we will show how theoretical modelling of the temperature dependent paramagnetic susceptibility signal could be used as a proxy to produce curves of "effective paramagnetic molar concentration" of the dopant at different temperatures. This could potentially broaden the applicability of the technique described in [3] to an in-situ borehole setting where temperature varies with depth, as well as providing the theoretical background for the technique to be applied at different temperatures in the laboratory. The relationship between molar concentration and NMR T2 relaxation times of the paramagnetic dopant from [3] was then used to produce curves of NMR T2 times with temperature using our model "effective paramagnetic molar concentration" values. We will also show how the NMR T2 curves behave with depth by converting the temperature scale to depth using an appropriate geothermal gradient.

2 Theory and Methods

2.1 Modelling the dependence of magnetic susceptibility on temperature, porosity and pore fluid type

Magnetic susceptibility is usually expressed in terms of magnetic susceptibility per unit volume k as:

$$k = J/H \qquad (1)$$

or in terms of magnetic susceptibility per unit mass χ as:

$$\chi = M/H = k/\rho \qquad (2)$$

where J is the magnetization per unit volume, M is the magnetization per unit mass, H is the applied external magnetic field, and ρ is the density of the material.

The temperature dependence of magnetic susceptibility per unit volume or per unit mass for a paramagnetic mineral is given by the Curie equation:

$$k = C_v/T \text{ or } \chi = C_m/T \qquad (3)$$

where C_v and C_m are the mineral specific Curie constants for volume magnetic susceptibility or mass magnetic susceptibility respectively, and T is the temperature in Kelvin. Knowing the volume magnetic susceptibility (VMS) or the mass magnetic susceptibility (MMS) at room temperature then **Equation (3)** allows us to construct curves of VMS or MMS with temperature. This can be done for a single paramagnetic mineral, or for a combination of paramagnetic minerals if one knows the proportions of the minerals, or for a mixture of paramagnetic and diamagnetic minerals (since the magnetic susceptibility of diamagnetic minerals is temperature independent). In the present study we will first model the temperature dependence of magnetic susceptibility for simple two component mixtures comprising of a paramagnetic mineral (illite clay) and a diamagnetic mineral (quartz). We chose this combination since these minerals are often the two key components in sandstones and shales. For volume magnetic susceptibility the total measured signal of this mineral mixture is given by [4]:

$$k_T = \{(F_I)\,(k_I)\} + \{(1-F_I)\,(k_Q)\} \qquad (4)$$

where k_T is the total volume magnetic susceptibility of the mixture, F_I is the illite fraction per unit volume, $(1-F_I)$ is the quartz fraction per unit volume, and k_I and k_Q are the volume magnetic susceptibilities of illite (41×10^5 SI [5]) and quartz (-1.64×10^5 SI [6, 7]) respectively. In our models we vary the fractions of illite and quartz, and the value of k_I will be temperature dependent, but the value of k_Q will be temperature independent. Likewise there is a similar expression for mass magnetic susceptibility as follows [8]:

$$\chi_T = \{(F_I)\,(\chi_I)\} + \{(1-F_I)\,(\chi_Q)\} \qquad (5)$$

where χ_T is the total mass magnetic susceptibility of the mixture, F_I is the illite fraction per unit volume, $(1-F_I)$ is the quartz fraction per unit volume, and χ_I and χ_Q are the mass magnetic susceptibilities of illite (15×10^8 m^3 kg^{-1} [5]) and quartz (-0.62×10^8 m^3 kg^{-1} [6, 7]), respectively. Again we can vary the fractions of illite and quartz, and the value of χ_I will be temperature dependent, but the value of χ_Q will be temperature independent.

We also modelled the effect of porosity simply by decreasing the total magnetic susceptibility in **Equations**

(4) and **(5)** by the chosen porosity fraction, and added an extra term for the fluid in the pore space. In our model examples to model different porosities we chose North Sea Forties field formation water to fully saturate (i.e., 100% saturation) the pore space. The mass magnetic susceptibility and volume magnetic susceptibility of the Forties field formation water is given in **Table 1** [6, 9].

Table 1. Magnetic susceptibility data for different Forties field (North Sea) reservoir fluids [6, 9].

Fluids	**Mass magnetic susceptibility (10^{-8} m^3 kg^{-1})**	**Volume magnetic susceptibility (10^{-6} SI)**
Formation water	-0.8729	-9.121
Crude oil	-1.0206	-8.134
Crude oil desalted	-1.0072	-8.163
Gasoline stabilized	-1.0744	-7.018
Kerosine	-0.9764	-7.991
Light gas oil	-0.9987	-8.277
Vacuum gas oil	-0.9788	-8.437
Heavy gas oil	-0.9861	-8.535

We also modelled the effects of other fluid types (all from the Forties field) in the pore space. Again we decreased the total magnetic susceptibility in **Equations (4)** and **(5)** by the chosen porosity fraction, and added an extra term for the fluid in the pore space. The magnetic susceptibility values for the different fluids modelled are given in **Table 1** and are based on previously published data [6, 9]. The mass magnetic susceptibility values of these fluids are the volume magnetic susceptibility divided by the density (**Equation (2)**). The density values are given in **Table 2** [6].

Table 2. Density data for different Forties field (North Sea) reservoir fluids [6].

Fluids	**Density (kg m^{-3})**
Formation water	1044.9
Crude oil	797.0
Crude oil desalted	810.4
Gasoline stabilized	653.2
Kerosine	818.4
Light gas oil	828.7
Vacuum gas oil	862.0
Heavy gas oil	865.5

2.2 Modelling the temperature dependent magnetic susceptibility of a paramagnetic dopant $MnCl_2$

In the study of reference [3] different molar concentrations of $MnCl_2$ were added to the brine phase in a carbonate sample to act as a paramagnetic dopant in order to separate out the NMR T2 relaxation time brine and oil peaks. Their study, however, was restricted to laboratory NMR measurements at room temperature. Since the dopant is paramagnetic then temperature dependent magnetic susceptibility modelling of concentrations of $MnCl_2$ similar to those described in **section 2.1** potentially allows the technique from [3] to be used more extensively as follows:

1. In a borehole setting where temperature changes with depth.
2. In laboratory heating and cooling experiments.

Therefore we firstly modelled the temperature dependent magnetic susceptibility of similar molar concentrations of $MnCl_2$ to those of [3] using **Equation (3)**. We then used the modelled magnetic susceptibility curves as a proxy to produce curves of "effective paramagnetic molar concentration" with temperature by normalising the magnetic susceptibility values to the value at room temperature (20ºC) for the 1 M curve. Thus the "effective paramagnetic molar concentration" at 20ºC for the 1 M curve was taken to be 1M, and all values at higher temperatures than 20ºC on this curve will have a lower "effective paramagnetic molar concentration" and conversely all values at lower temperatures than 20ºC on this curve will have a higher "effective paramagnetic molar concentration." Curves with lower initial molar concentrations at room temperature will act in a similar way, but have lower overall values.

We then converted the "effective paramagnetic molar concentration" scale to an NMR T2 relaxation time using data from reference [3]. **Figure 1** shows the NMR T2 peaks for the brine phase with the added $MnCl_2$ dopant, compared to the peaks for the oil phase, for a carbonate saturated sample [3]. We have highlighted the $MnCl_2$ doped brine peaks with red arrows. The four different peaks result from four different molar concentrations of $MnCl_2$ as indicated. The peaks with the longer T2 times (without the red arrows) are all due to the oil phase. For the four $MnCl_2$ doped brine peaks we plotted the $MnCl_2$ molar concentrations against NMR T2 time (**Figure 2**) and obtained a power law relationship as follows:

$$y = 0.0746\, x^{-1.513} \tag{6}$$

where y corresponds to molar concentration and x corresponds to NMR T2 relaxation time. Solving for x as follows:

$$x = \frac{0.0746^{\frac{1}{1.513}}}{y^{\frac{1}{1.513}}} \tag{7}$$

allows one to calculate NMR T2 relaxation times from our values of "effective paramagnetic molar concentration" which were derived from the temperature dependent magnetic susceptibility data. This allowed us to then produce curves of NMR T2 time against temperature, which can also be converted into NMR T2 time with depth for borehole applications by using an appropriate geothermal gradient or from direct temperature log measurements.

3 Results and discussion

3.1 Modelling the temperature dependence of paramagnetic susceptibility: an example with a two component mineral mixture

We first present the temperature dependence of two component mineral mixtures comprising quartz (a diamagnetic mineral) and illite (a paramagnetic mineral). We chose this example as it is a simple approximation to some sandstones and shales, depending upon the relative contents of each mineral. The illite has a temperature dependent magnetic susceptibility given by the Curie equation (**Equation (3)**), whereas the magnetic susceptibility of the quartz is temperature independent. **Figure 3** shows the variation of volume magnetic susceptibility (VMS) with low temperature for various illite contents (ranging between 1-10%), and so it is mainly applicable for clean to muddy sandstones. The curves show how the magnetic susceptibility increases with decreasing temperature, and thus the potential of cooling experiments in the laboratory for identifying small concentrations of illite that may not be apparent from traditional room temperature measurements.

Figure 4 shows the variation of VMS with higher temperatures for the same illite contents as **Figure 3**. Both **Figures 3** and **4** can be used to quantify the illite and quartz contents (by comparing the theoretical curves from these figures with experimental temperature dependent VMS measurements), if these two minerals are known to be the two main minerals in the rock sample (e.g., from thin section analysis, or X-ray diffraction etc.). **Figure 4**, and similar types of theoretical curves for other paramagnetic minerals and mixtures, is potentially useful for correctly quantifying mineral content from borehole magnetic susceptibility measurements where temperature generally increases with depth. A borehole temperature profile is often measured, or can be generated at each depth if one knows the local geothermal gradient.

We previously undertook similar modelling for mass magnetic susceptibility (MMS) for an identical two component system [1, 2]. However, VMS is more relevant for borehole measurements as we mentioned earlier. We have also modelled the VMS and MMS curves with temperature for higher concentrations illite, but have not shown those due to space limitations in the present paper.

3.2 Modelling the effects of porosity and pore fluid type on temperature dependent magnetic susceptibility: examples for shale and muddy sand

Figure 5 shows the effect of different porosities (ranging from 0-40% porosity) on the volume magnetic susceptibility over a temperature range of 20ºC to just under 450ºC for model shale and muddy sandstone samples. The shale samples have an illite to quartz ratio of 4:1, whilst for the muddy sandstone samples the ratio is 1:10. The higher porosity values for the simulated "shale" samples we recognize are unrealistic (as shale samples normally have lower porosities), but we included them merely for modelling purposes to compare with similar porosities for the muddy sandstone. All the model samples are assumed to be 100% saturated with Forties field formation water, whose volume magnetic susceptibility is given in **Table 1**. **Figure 5** clearly shows that as the porosity increases the volume magnetic susceptibility decreases.

Figure 6 shows the effects of different Forties field fluids (7 hydrocarbons and 1 formation water, whose magnetic susceptibility values are given in **Table 1**) on the volume magnetic susceptibility over the same temperature range as for **Figure 5** for a simulated sample with an illite to quartz ratio of 4:1 and a porosity of 40%. We used a high porosity value in order to enhance the effects of the different fluids. However, **Figure 6** shows that the different fluids have almost the same effect on the results, with only slight differences between them. Lower values of porosity exhibited even smaller differences between the fluids.

Figures 7 and **8** show similar plots for the effects of porosity and pore fluid porosity on identical model samples to **Figures 5** and **6**, but this time for mass magnetic susceptibility. **Figure 7** shows that the effect of porosity on the mass magnetic susceptibility appears to be slightly less within each sample type (shale or muddy sandstone) compared to the volume magnetic susceptibility. This might be expected and can be explained simply because volume magnetic susceptibility will decrease with increasing porosity for the samples considered, whilst for mass magnetic susceptibility the masses (and densities) of the samples are also decreasing with increasing porosity, which has the effect of causing less of a variation in the mass magnetic susceptibility values for a particular sample type (since the parameters k and ρ are both decreasing in **Equation (2)** and so the ratio is less affected).

Figure 8 shows the effects of the different Forties field fluids on the mass magnetic susceptibility over the same temperature range as the equivalent plot for volume magnetic susceptibility (**Figure 6)**. In this case there is slightly more separation between the different fluid curves compared to **Figure 6** for the volume magnetic susceptibility case. This is largely due to the different densities of the fluids (**Table 2**), which affect the mass magnetic susceptibility (**Equation (2)**).

3.3 Modelling the temperature dependent behaviour of a paramagnetic dopant: extending its use for borehole applications and laboratory heating or cooling experiments

Figure 9 shows the modelled temperature dependence of magnetic susceptibility for different molar concentrations of manganese chloride ($MnCl_2$) in aqueous solutions, using the methodology described in **section 2.2**. We used the same molar concentrations that were used in Mitchell et al's [3] study, where $MnCl_2$ was used as a paramagnetic dopant added to the brine phase. The magnetic susceptibility of a 1 molar (1M) solution of $MnCl_2$ was taken to be 14350 x 10^{-6} cm^3 mol^{-1} at a

room temperature of 20ºC [10]. The variations in the magnetic susceptibility with temperature can potentially be used as a proxy for an "effective paramagnetic molar concentration" of the $MnCl_2$ with temperature. **Figure 10** shows a plot of this "effective paramagnetic molar concentration" with temperature, which is derived by normalising the molar magnetic susceptibility values in **Figure 9** to the value at room temperature (20ºC) for the 1 M curve. This means that in **Figure 10** the "effective paramagnetic concentration" at 20ºC for the 1 M curve is 1M (as detailed in **section 2.2**).

Since Mitchell et al [3] reported values of the NMR T2 relaxation time for the four different molar concentrations of $MnCl_2$ (see **Figure 1**) we identified a power law relationship between molar concentration of $MnCl_2$ and NMR T2 relaxation time of the doped brine (see **Figure 2**), as detailed in **section 2.2**. This subsequently allowed us to associate each of our "effective paramagnetic molar concentrations" from **Figure 10** with corresponding NMR T2 values, using **Equations (6)** and **(7)** as described in **section 2.2**. This then enabled us to produce plots of NMR T2 versus temperature (**Figure 11**) for the four initial molar concentrations of $MnCl_2$ at room temperature (i.e., 0.005 M, 0.04 M, 0.3 M and 1 M at 20ºC). The results show that as the temperature increases the NMR T2 time increases for each molar concentration. This data can be used to quantify how the NMR T2 time for the $MnCl_2$ doped brine should vary with depth in a borehole setting where temperature is generally increasing with increasing depth.

In order to provide an example of a relevant depth plot we used an appropriate geothermal gradient from the Middle East, since this was where Mitchell et al's [3] carbonate samples came from that were saturated with brine containing the different $MnCl_2$ concentrations. We used a geothermal gradient of 35^0C/km [11] to convert temperature to depth and produced plots of NMR T2 time with depth (**Figure 12**) for the four initial molar concentrations of $MnCl_2$ at room temperature (i.e., 0.005 M, 0.04 M, 0.3 M and 1 M at 20ºC). **Figure 12** illustrates that as the depth increases the NMR T2 time for the $MnCl_2$ doped brine increases.

Figures 11 and **12** demonstrate the potential of the technique proposed by Mitchell et al [3] to now also be applied to a borehole setting. One implication of **Figures 11** and **12** is that as temperature and depth increase, then the separation of the NMR T2 peaks between the $MnCl_2$ doped brine and the oil will become less. Another interesting implication of **Figure 11** is that cooling the $MnCl_2$ dopant below room temperature will decrease the NMR T2 time, and thus increase the separation between the NMR T2 peaks of the $MnCl_2$ doped brine and the oil. Thus, in a laboratory setting, cooling the sample saturated with the $MnCl_2$ doped brine and oil (even by just a few degrees below room temperature) will potentially provide an even better separation of the NMR T2 peaks, providing a further improvement over the results obtained by Mitchell et al [3], which were taken at room temperature.

4 Conclusions

The following overall conclusions can be drawn:

1. Model template curves were constructed of the temperature dependence of volume magnetic susceptibility for different mixtures of a paramagnetic and a diamagnetic mineral. The curves allow the paramagnetic and diamagnetic mineral contents to be quantified by directly comparing them with experimental laboratory or borehole volume magnetic susceptibility measurements. The "high" temperature template curves (**Figure 4**) are potentially useful both for laboratory heating experiments, and borehole magnetic susceptibility measurements where temperature usually increases with increasing depth. The "low" temperature template curves (**Figure 3**) are especially useful for laboratory cooling experiments where the increased paramagnetic signal allows small concentrations of paramagnetic minerals to be identified that may otherwise be missed from traditional room temperature measurements. (We previously [1] showed some comparisons between our initial template curves for mass magnetic susceptibility and experimental laboratory measurements for some shoreface and turbidite samples for the high temperature case).

2. The effect of porosity on the temperature dependent magnetic susceptibility curves for different paramagnetic + diamagnetic mixtures showed that increased porosity caused the magnetic susceptibility to decrease in the modelled samples, since the amount of the paramagnetic mineral (which has a positive magnetic susceptibility) is decreased. Porosity appears to have less of an effect on the mass magnetic susceptibility compared to the volume magnetic susceptibility, mainly because the mass and density also decrease with increasing porosity. The mass magnetic susceptibility is the volume magnetic susceptibility divided by the density (k/ρ), and so if both k and ρ are decreasing the ratio (the mass magnetic susceptibility) may be less affected compared to k (the volume magnetic susceptibility) alone.

3. Different pore fluids were shown to have little effect on the volume magnetic susceptibility, and some slight (though minor) effect on the mass magnetic susceptibility. The reason for the latter is mainly due to the different densities of the fluids, which affect the mass magnetic susceptibility.

4. Modelling the temperature dependence of a paramagnetic dopant ($MnCl_2$ in the aqueous phase) allows one to construct plots of "effective paramagnetic molar concentration" with temperature. Using previous data from Mitchell et al [3] that related the $MnCl_2$ doped brine concentration to NMR T2 relaxation time, we could construct plots of NMR T2 time versus temperature for the $MnCl_2$ dopant from our "effective paramagnetic

molar concentration" versus temperature curves. Using an appropriate geothermal gradient, we could also produce typical plots of NMR T2 time with depth for the $MnCl_2$ doped brine phase. The modelled results potentially increase the application of Mitchell et al's [3] technique (which used the dopant in the brine in order to separate out the brine NMR T2 peak from the oil NMR T2 peak, but only at room temperature in the laboratory) to an in-situ borehole setting where the temperature varies with depth. One consequence of the modelling for borehole applications is that as temperature and depth increase the separation of the NMR T2 times between the $MnCl_2$ doped brine and the oil signal will become less.

5. A further implication of the $MnCl_2$ dopant modelling is that cooling the sample with the $MnCl_2$ dopant (even by just a few degrees below room temperature) will decrease the NMR T2 time of the doped brine, which would potentially provide an even greater separation between the $MnCl_2$ doped brine and oil NMR T2 times, thus further improving the results obtained by Mitchell et al [3] that were undertaken at room temperature.

D. K. P. thanks the Natural Sciences and Engineering Research Council of Canada (NSERC) for a Discovery Grant. Eric Withjack and Holger Ott are thanked for their constructive review comments, which helped improve the manuscript.

5 List of abbreviations

MMS	Mass Magnetic Susceptibility
NMR	Nuclear Magnetic Resonance
T2	NMR T2 transverse relaxation time
VMS	Volume Magnetic Susceptibility

6 References

1. A. Ali and D. K. Potter. Model templates for quantifying permeability controlling paramagnetic clay minerals at in situ reservoir temperatures. *Proceedings of the 2011 International Symposium of the Society of Core Analysts***,** *18-21 September 2011,* Austin, Texas, USA. Paper SCA2011-047 (2011)
2. A. Ali and D. K. Potter. Temperature dependence of the magnetic properties of reservoir rocks and minerals and implications for in situ borehole predictions of petrophysical parameters. Geophysics, **77** (no.3), 211-221 (2012)
3. P. Mitchell, L. Gromala and M. Siddiqui. The use of paramagnetic dopants in optimizing the accuracy of critical and residual oil saturation determination. *Proceedings of the 2017 International Symposium of the Society of Core Analysts, 27 August – 1 September 2017,* Vienna, Austria. Paper SCA2017-063 (2017)
4. T. H. To and D. K. Potter. Comparison of high resolution probe magnetics, X-ray fluorescence and permeability on core with borehole spectral gamma ray and spontaneous potential in an oil sand well. *Proceedings of the 2021 International Symposium of the Society of Core Analysts,* (Online 13-16 September 2021), Paper SCA2021-035 (2021)
5. C. P. Hunt, B. M. Moskowitz and S. K. Banerjee. Magnetic properties of rocks and minerals. In: *Rock Physics and Phase Relations: A Handbook of Physical Constants*, T. J. Ahrens (Ed.). American Geophysical Union Reference Shelf 3, 189-204 (1995)
6. O. P. Ivakhnenko. Magnetic analysis of petroleum reservoir fluids, matrix mineral assemblages and fluid-rock interactions. PhD thesis, Heriot-Watt University, Institute of Petroleum Engineering, Edinburgh, UK, pp. 210 (2006)
7. D. K. Potter, T. M. AlGhamdi, and O. P. Ivakhnenko. Sensitive carbonate reservoir rock characterization from magnetic hysteresis curves and correlation with petrophysical properties. Petrophysics, **52** (issue 1), 50-57 (2011)
8. D. K. Potter. Magnetic susceptibility as a rapid, non-destructive technique for improved petrophysical parameter prediction. Petrophysics, **48** issue 3), 191-201 (2007)
9. O. P. Ivakhnenko and D. K. Potter. Magnetic susceptibility of petroleum reservoir fluids. Physics and Chemistry of the Earth, **29**, 899-907 (2004)
10. J. R. Rumble, ed. *CRC Handbook of Chemistry and Physics*, 102nd Edition (Internet Version 2021), CRCPress/Taylor and Francis, Boca Raton, Fl (2021) https://hbcp.chemnetbase.com/faces/documents/04_08/04_08_0001.xhtml
11. Swart, P.K., Cantrell, D.L., Arienzo, M.M. and Murray, S.T. Evidence for high temperature and ^{18}O-enriched fluids in the Arab-D of the Ghawar Field, Saudi Arabia. Sedimentology, **63**, 1739-1752 (2016)

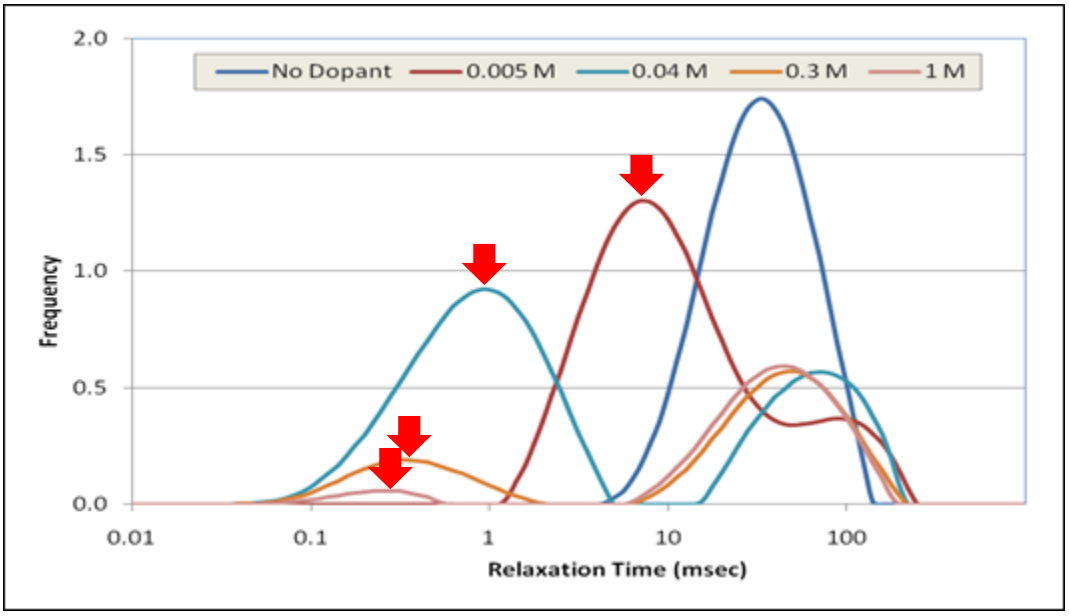

Fig. 1. Separation of brine and oil NMR T2 relaxation time peaks in a carbonate sample for different molar concentrations of paramagnetic $MnCl_2$ dopant added to the brine phase. The vertical "Frequency" axis is in arbitrary units. The red arrows indicate the peaks for the brine + $MnCl_2$ dopant and are the shorter relaxation times. The peaks for the oil phase are the ones with the longer relaxation times, without the red arrows. (Modified from Mitchell et al [3]).

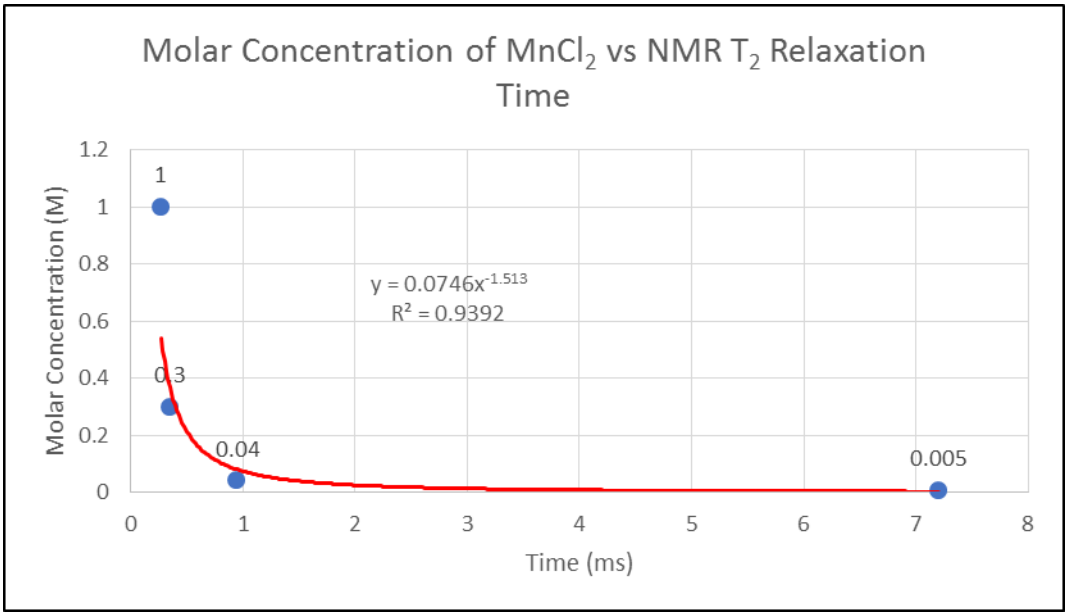

Fig. 2. Plot of the molar concentration of paramagnetic $MnCl_2$ dopant versus NMR T_2 relaxation time of the doped brine derived from **Figure 1**. The red regression line shows a power law fit to the data with a coefficient of determination of $R^2 = 0.94$. The regression equation shown (see also **section 2.2** of the text) was used in conjunction with the "effective paramagnetic molar concentration" of **Figure 10** to produce the NMR T2 relaxation times for the doped brine shown in **Figures 11** and **12**.

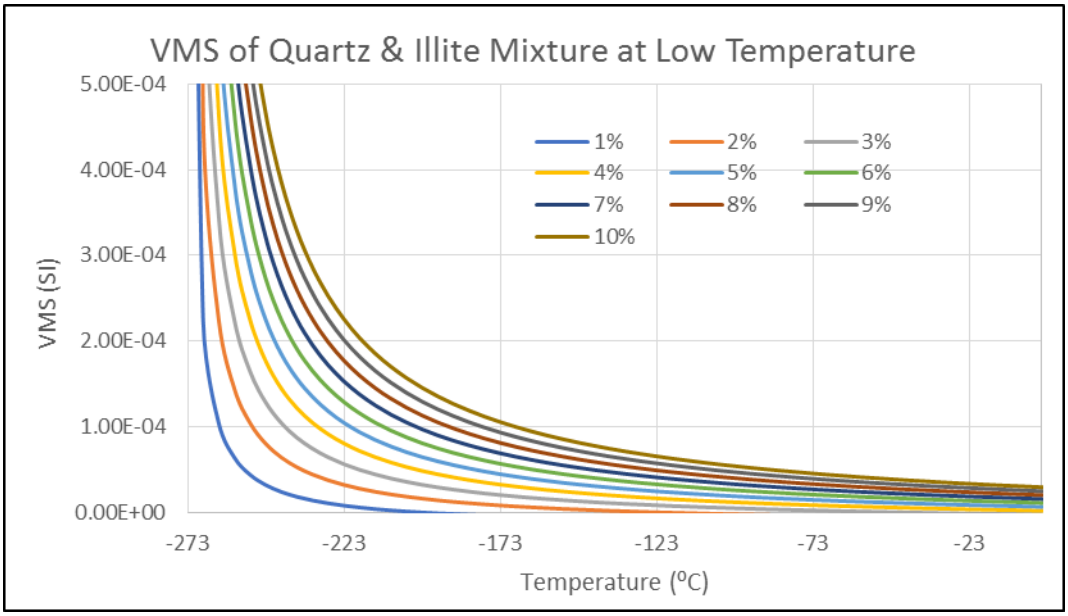

Fig. 3. Model template curves showing the dependence of volume magnetic susceptibility (VMS) on temperature for low temperature conditions for varying mixtures of illite ranging from 1-10% (shown in the legend) + quartz ranging, respectively, from 99-90% (so the total percentage of the two minerals is 100% for each curve). Illite is paramagnetic and so its VMS is temperature dependent in accordance with the Curie equation (**Equation (3)** in **section 2.1**), whereas quartz is diamagnetic and its VMS is temperature independent. Note that these curves do not include porosity (i.e., porosity = 0%), but **Figures 5** and **7** show VMS and MMS (mass magnetic susceptibility) results for different porosities. The curves in **Figure 3** are potentially useful for identifying and quantifying small amounts of illite (and similar curves can be produced for other paramagnetic minerals) by comparing with laboratory low temperature dependent VMS measurements. The increased VMS signal at low temperatures could be particularly useful for identifying minute amounts of illite that may not be evident from traditional room temperature measurements.

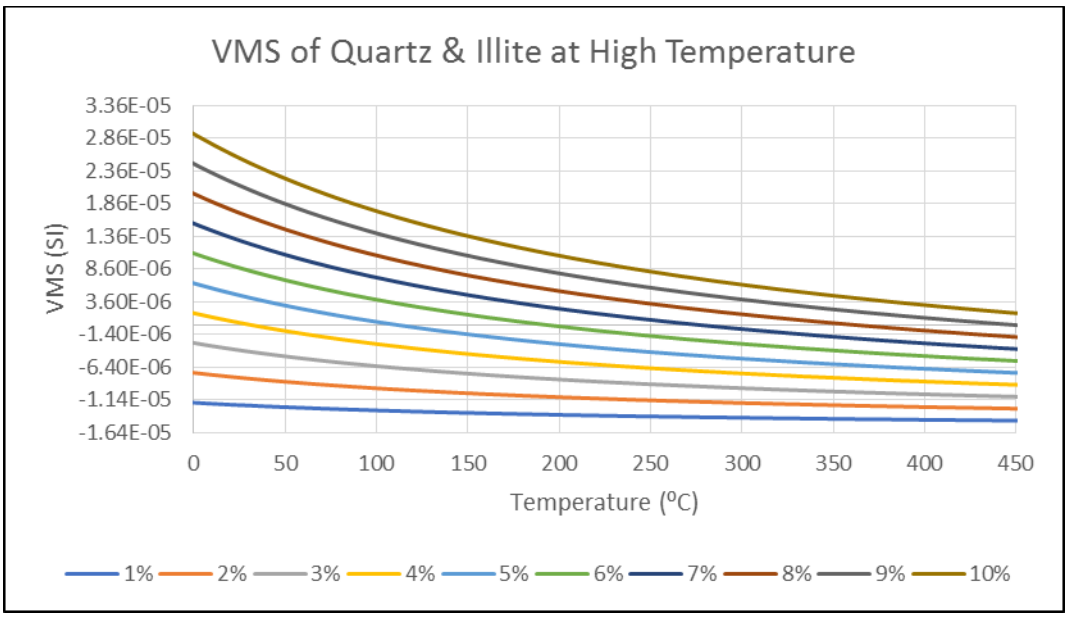

Fig. 4. Model template curves showing the dependence of volume magnetic susceptibility (VMS) on temperature for high temperature conditions for varying mixtures of illite ranging from 1-10% (shown in the legend) + quartz ranging, respectively, from 99-90%. These curves are potentially useful for quantifying the mineral contents in samples with similar mineral components by comparing with laboratory temperature dependent VMS measurements, or with borehole VMS data. These curves do not include porosity (i.e., porosity = 0%), but **Figures 5** and **7** show VMS and MMS (mass magnetic susceptibility) results for different porosities.

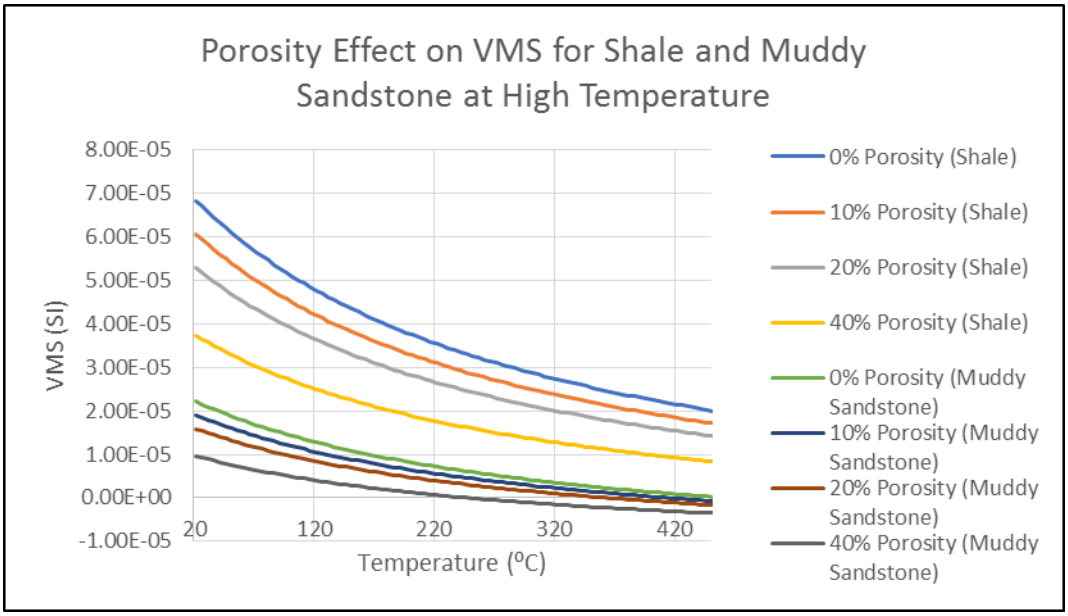

Fig. 5. Model curves of volume magnetic susceptibility (VMS) versus temperature (high temperature range) for varying porosity values in simulated shale and muddy sandstone samples 100% saturated with Forties Field formation water (see **Table 1**). An illite to quartz ratio of 4:1 was used for the simulated shale samples, whilst an illite to quartz ratio of 1:10 was used for the simulated muddy sandstone samples.

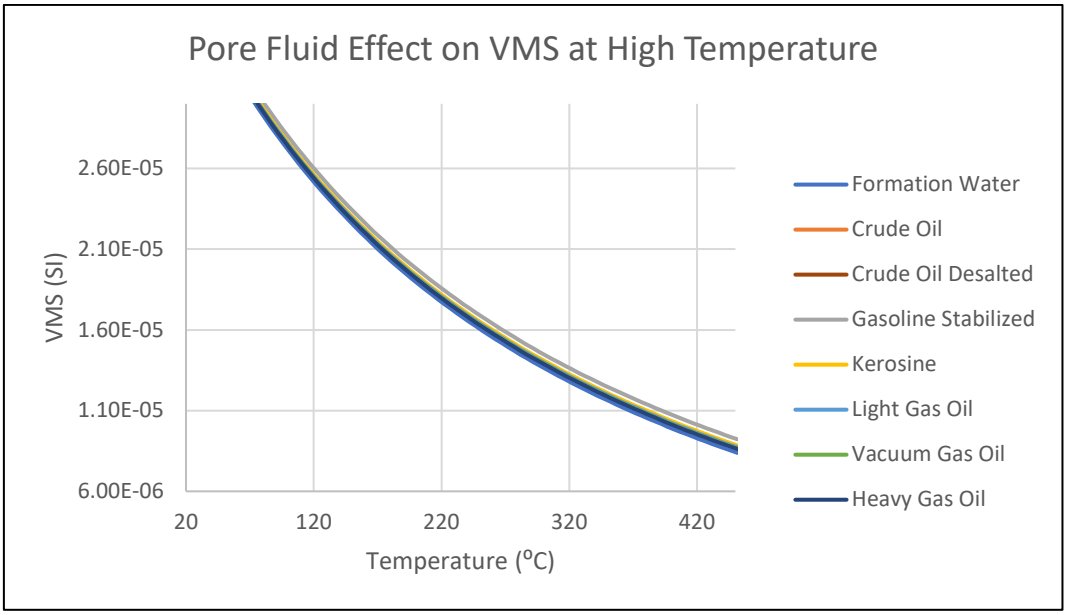

Fig. 6. Model curves of volume magnetic susceptibility (VMS) versus temperature (high temperature range) for a simulated shale composition (illite to quartz ratio of 4:1) 100% saturated with different Forties Field reservoir fluids in the pore space (see **Table 1**). The porosity was taken to be 40% in this example. We recognize this is unrealistic for a shale, but we used a high porosity value in order to enhance the effects of the different fluids. Lower values of porosity exhibited even smaller differences between the fluids.

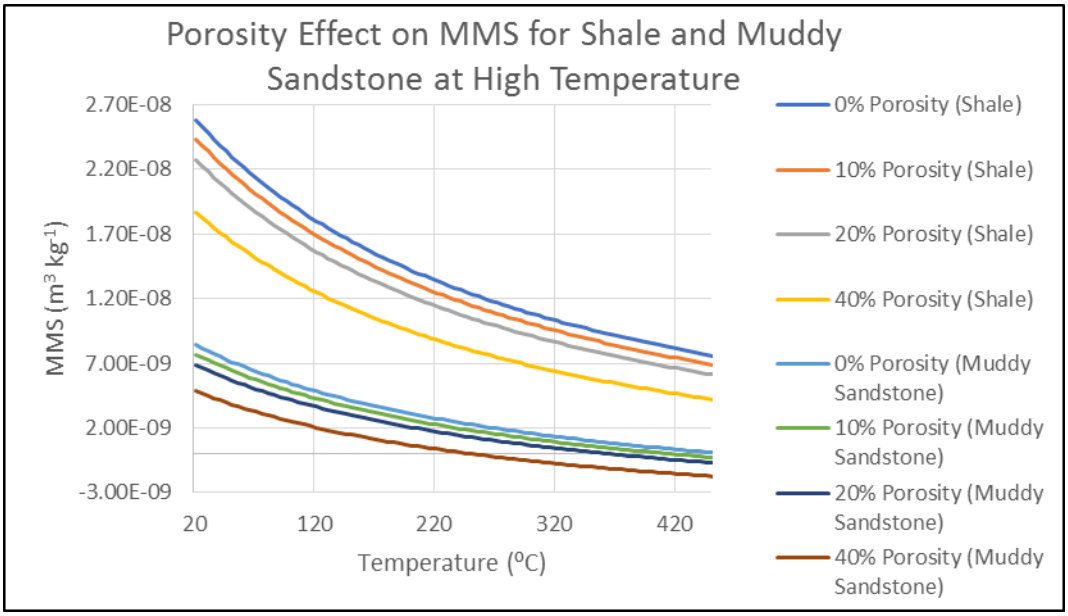

Fig. 7. Model curves of mass magnetic susceptibility (MMS) versus temperature (high temperature range) for varying porosity values in simulated shale and muddy sandstone samples 100% saturated with Forties Field formation water (see **Table 1**). An illite to quartz ratio of 4:1 was used for the simulated shale samples, whilst an illite to quartz ratio of 1:10 was used for the simulated muddy sandstone samples.

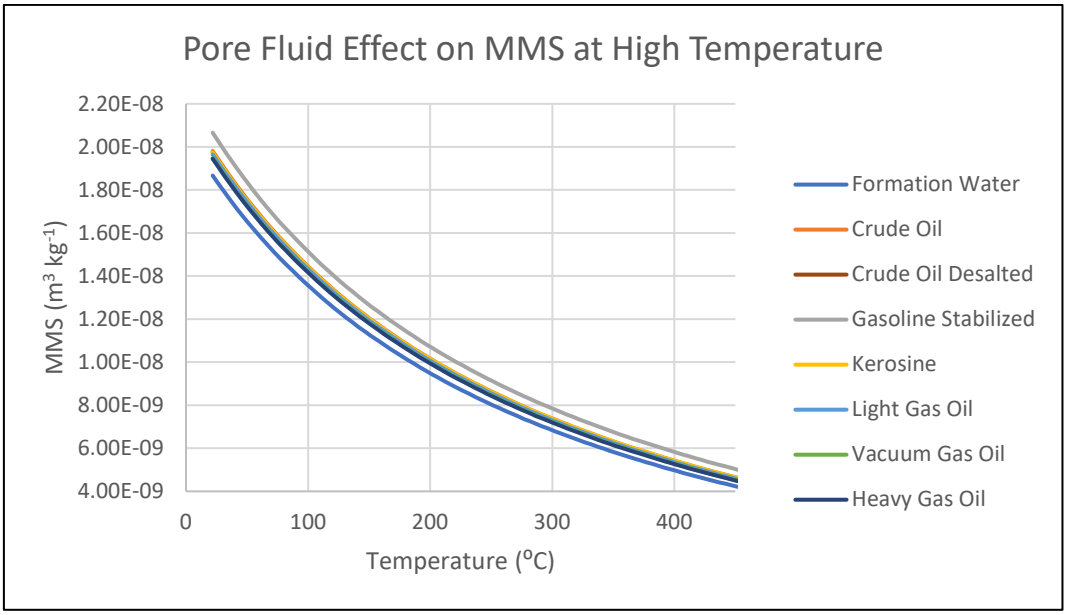

Fig. 8. Model curves of volume magnetic susceptibility (VMS) versus temperature (high temperature range) for a simulated shale composition (illite to quartz ratio of 4:1) 100% saturated with different Forties Field reservoir fluids in the pore space (see **Table 1**). The porosity was taken to be 40% in this example. Again we recognize this is unrealistic for a shale, but we used a high porosity value in order to enhance the effects of the different fluids. The slightly greater separation of the curves compared to the VMS results of **Figure 6** are mainly due to differences in density (see **Table 2**) since mass magnetic susceptibility is the volume magnetic susceptibility divided by the density.

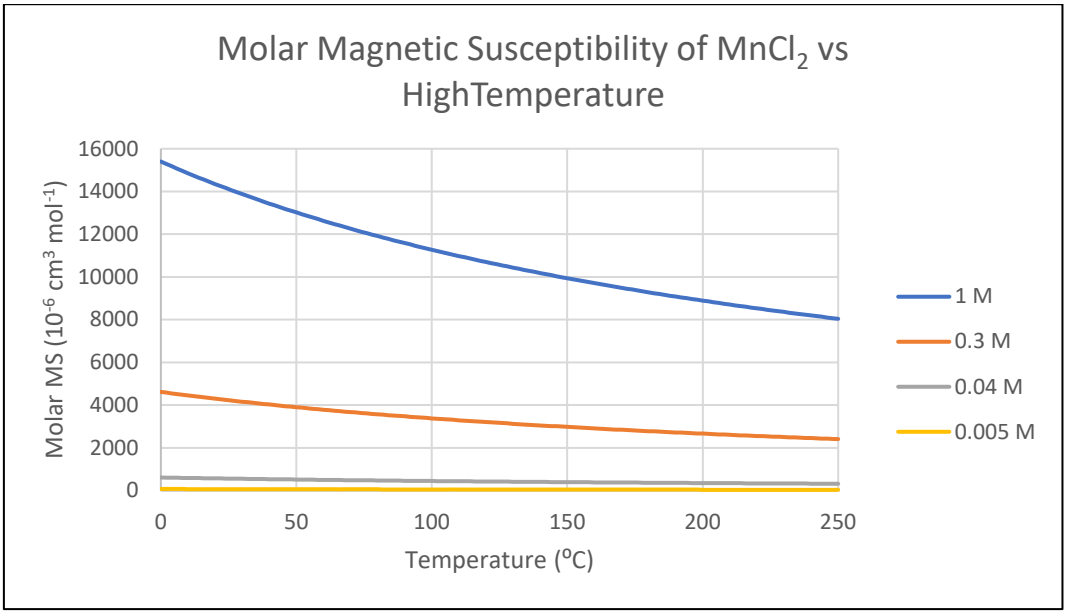

Fig. 9. Model curves of molar magnetic susceptibility calculated for the different initial molar concentrations of the paramagnetic dopant $MnCl_2$ used by [3] (1 M, 0.3 M, 0.04 M and 0.005 M at room temperature of 20ºC) versus temperature for the high temperature range. For the modelling we used a molar magnetic susceptibility value of 14350 x 10^{-6} cm^3 mol^{-1} at a room temperature of 20ºC [10] for a 1 molar (1M) solution of $MnCl_2$.

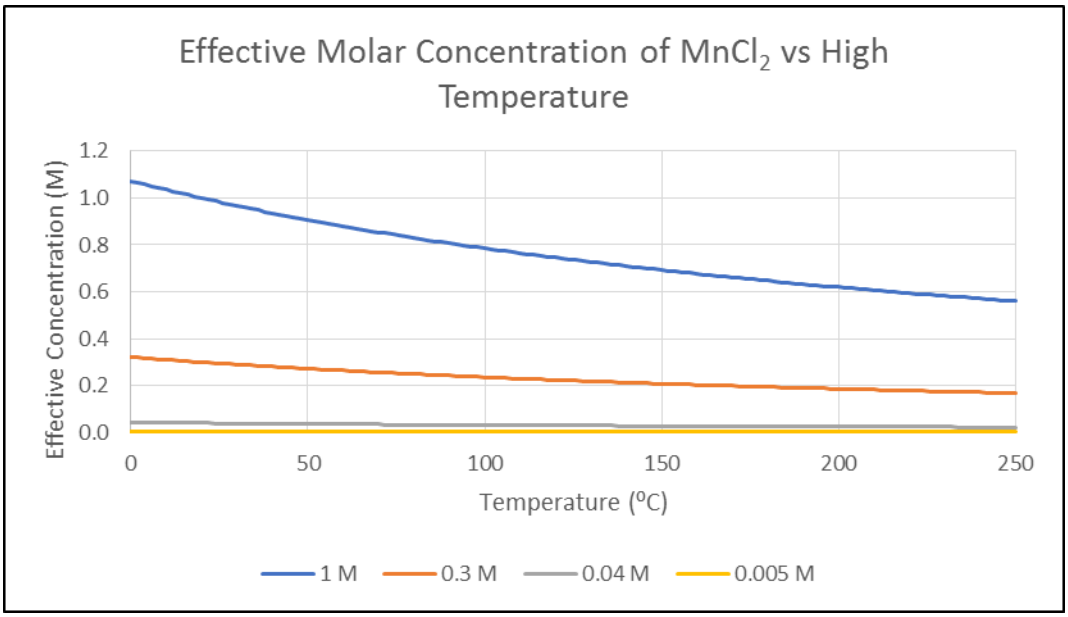

Fig. 10. Model curves of the effective paramagnetic molar concentrations of $MnCl_2$ versus temperature for the high temperature range. The effective paramagnetic molar concentration values were derived by normalising the molar magnetic susceptibility values in **Figure 9** to the value at room temperature (20ºC) for the 1 M curve (i.e., the effective paramagnetic molar concentration at 20ºC for the 1 M curve is 1M).

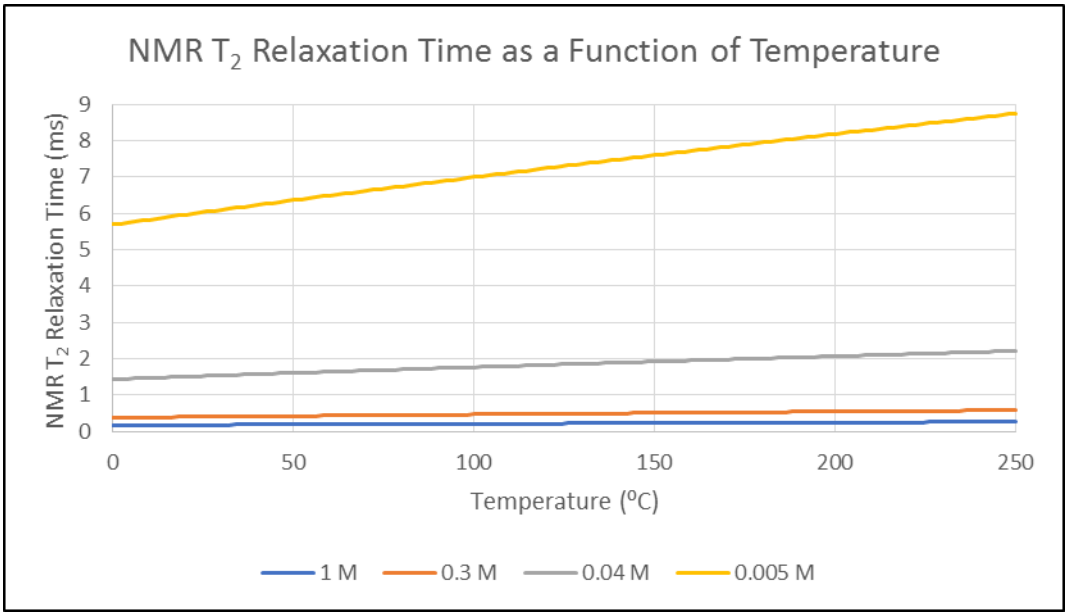

Fig. 11. Model NMR T2 relaxation times of the doped brine for the different initial molar concentrations of the paramagnetic dopant $MnCl_2$ (1 M, 0.3 M, 0.04 M and 0.005 M at a room temperature of 20ºC) versus temperature for the high temperature range. The NMR T2 times were derived from the relationship between the molar concentrations and NMR T2 times for the doped brine shown in **Figure 2** (the relationship is also shown in **Equations (6)** and **(7)**) using the effective paramagnetic molar concentrations from **Figure 9**.

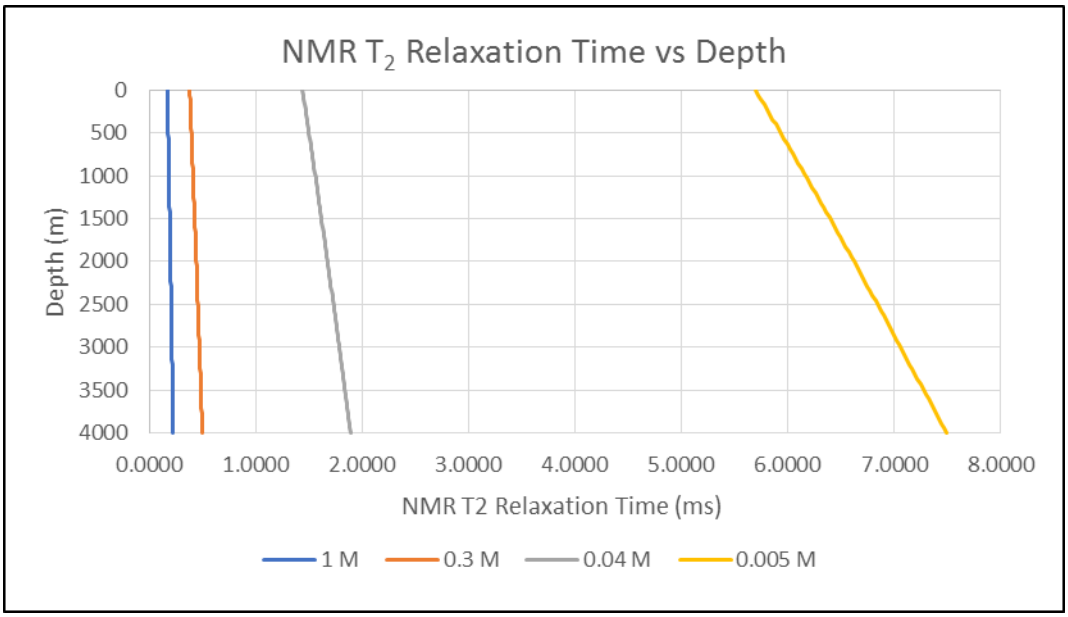

Fig. 12. Model NMR T2 relaxation times of the doped brine for the different initial molar concentrations of the paramagnetic dopant $MnCl_2$ (1 M, 0.3 M, 0.04 M and 0.005 M at a room temperature of 20ºC) versus depth. The depth scale was derived from the temperature scale of **Figure 11** using a geothermal gradient of 35^0C/km [11], which is relevant to the Middle East (specifically Saudi Arabia) where the carbonate samples in Mitchell et al's [3] study originated.